

SUPPLEMENTAL INFORMATION

A novel GRK2/HDAC6 interaction modulates cell spreading and motility

VanesaLafarga^{1,2}, Ivette Aymerich¹, Olga Tapia³,
Federico Mayor, jr.^{1,2,*} and Petronila Penela^{1,2,*}

¹ Departamento de Biología Molecular and Centro de Biología Molecular “Severo Ochoa”, Universidad Autónoma de Madrid, 28049 Madrid, Spain,

² Instituto de Investigación Sanitaria La Princesa, 28006 Madrid, Spain

³ Department of Anatomy and Cell Biology, University of Cantabria-IFIMAV, Santander, Spain

Supplemental Figure Legends

Fig. S1. Silencing of either GRK2 expression or activity induces tubulin acetylation and reduces motility. (A-C) MEFs derived from wt or hemizygous GRK2 mice were infected with an adenoviral-GRK2 shRNA construct or adenoviral-Lamin shRNA construct as a control. (A) Protein from the polymerized fraction of MTs was obtained as described in Materials and methods and levels of acetylated α -tubulin and total α -tubulin analyzed by western blot. (B) The same cells were seeded on transwell filters coated with 20 μ g/ml FN and their migration rates determined as described in Materials and methods. Levels of GRK2 expression upon silencing were analyzed by western blot (C). Data (mean \pm SEM) from two-three experiments are represented. *** $p < 0.001$, compared to wild-type control infected MEFs, unpaired two-tailed t-test. It is worth mentioning that Nicotinamide, an inhibitor of SIRT2 deacetylase (*North et al., 2003*), did not affect migration of wt or GRK2 +/- MEFs (data not shown), thus ruling out the involvement of deacetylases other than HDAC6 in these cells, in line with previous reports (*Gao et al., 2007*). **(D-E)** Gene-targeted inactivation of GRK2 inhibits fibroblast cell migration. Primary MEFs derived from homozygous GRK2-floxed embryos were infected with control or Cre-recombinase-expressing adenovirus. Levels of GRK2 expression and chemotactic motility towards FN were assessed as above. Data are mean \pm SEM from three independent experiments performed in duplicate. ** $p < 0.01$, compared to parental or control infected cells, unpaired two-tailed t-test. **(F)** HDAC6 protein levels are unaffected by altered GRK2 expression or functionality. Parental and HeLa cells stably transfected with either a control or a GRK2 silencing construct (shGRK2) or stably expressing GRK2 wt (Wt5), GRK2-S670A (A1) or GRK2-K220R (K1) mutants were analyzed for HDAC6 levels. Total α -tubulin serves as loading control. **(G)** Altered levels of GRK2 expression or kinase functionality do not modify the extent of tubulin poly-glutamylolation or tyrosination. Parental or HeLa cells stably expressing GRK2 wt (Hela-wt5), GRK2-S670A (Hela-A1) or GRK2-K220R (Hela-K1) were collected and lysed to detect by western blot the presence of tyrosinated and poly-glutamylated tubulin with specific antibodies. Blots are representative of 3 independent experiments. **(H)** GRK2 levels stimulate cellular motility of HeLa cells in a kinase-dependent manner. Migration of parental, HeLa-K1 or -wt5 cells was analyzed in wound healing assays as described in Materials and methods. At time 0 and 16 h after wounding, cells were analyzed using optical microscopy.

Dotted lines indicate the wound borders. Wound-closure after 16 hours of migration (filled area) was determined as percentage of the initial wound area and plotted. Data are mean \pm SEM of two independent experiments.

Fig.S2. The effect of GRK2 levels on cell migration is not mediated by HDAC6-dependent deacetylation of cortactin or altered HDAC6 binding to tubulin. (A, B)

Altered levels of GRK2 expression or kinase functionality do not modify the extent of cortactin acetylation. Cell lysates from parental and HeLa cells stably expressing GRK2 wt (Wt5), GRK2-S670A (A1) or GRK2-K220R (K1) mutants or silenced for GRK2 expression (shGRK2) were processed for cortactin immunoprecipitation and immune complexes were analyzed by immunoblot with a specific anti-acetyl-cortactin antibody as detailed in Material and methods. HeLa cells treated with TSA (1mM) for 12h serve as positive control of acetylated cortactin. A similar approach was conducted in HEK293 cells transiently transfected with different combinations of plasmids coding for HDAC6, flag-tagged cortactin-wt, GRK2-wt, GRK2-S670A or GRK2-K220R proteins. Data are mean \pm SEM from two independent experiments. Representative blots are shown. **(C, D)** GRK2-induced migration is insensitive to the acetylation status of cortactin. Parental and HeLa-wt5 cells were transiently co-transfected with the CD-8 antigen and wild-type cortactin (C) or different mutated constructs that mimic the deacetylation (cortactin-K9R) or acetylation (cortactin-K9Q) state of cortactin (D). After cell selection by using microbeads precoated with anti-CD8 antibody, cellular migration towards fibronectin was assessed. Cortactin expression levels were analysed by western blot. Presence of either extra cortactin-wt or cortactin-K9R, which efficiently binds to F-actin, stimulated HeLa cell motility, while expression of the F-actin binding-defective cortactin-K9Q mutant had an inhibitory effect. In contrast, neither over-expression of cortactin-wt nor mutated cortactin constructs altered the increased motility of HeLa-wt5 cells. Control cells in panels C and D refers to mock-transfected HeLa cells and cortactin-wt transfected cells, respectively. ** $p < 0.01$, compared to control cells, unpaired two-tailed t-test. **(E)** HDAC6 association to tubulin is not affected by the presence of extra GRK2 wt or mutant proteins. HEK293 cells were transfected with HDAC6 and GRK2 constructs as indicated and tubulin immunoprecipitates analyzed for the presence of HDAC6 and GRK2. Expression levels of these proteins in cell lysates were monitored with specific antibodies as described in Material and methods.

Fig. S3. HDAC6 and phosphorylated GRK2 at S670 co-localize at the membrane leading edge of migrating cells, an area that displays underneath an hypoacetylated microtubule network. HeLa-wt5 cells were plated in FN (10 μ g/ml)-coated dishes and scratched to promote wound healing as indicated in Materials and methods. After 16h of migration, cells were fixed and potential co-localization of acetylated α -Tubulin with HDAC6 or GRK2 (A) and of HDAC6 with pS670-GRK2 (B) was determined by confocal microscopy upon staining with specific antibodies. Arrows indicate the leading edge of migrating cells.

Fig. S4. Silencing of GRK2 expression accelerates cell spreading. HeLa cells stably expressing a GRK2 silencing construct (HeLa-shGRK2) were plated on cover slips coated with FN (10 μ g/ml), fixed at the indicated times and analyzed by confocal microscopy. The spreading area was quantified by morphometric analysis (A) and cells were triple-stained (B) for acetylated α -Tubulin (blue), α -Tubulin (green) and F-actin (Phalloidin, red) as described in Materials and methods.

Fig.S5. Both pattern of focal adhesions and formation of the F-actin network during cellular spreading are altered in the presence of GRK2-K220R or GRK2-S670A mutants. Parental or HeLa-K1, -A1 and -wt5 cells were kept in suspension for 2h and then allowed to adhere to coverslips coated with FN (10 μ g/ml) for 60 min before being fixed, stained for paxillin (A) or for F-actin with phalloidin (B) and analyzed by confocal microscopy. The presence of the GRK2 mutants strongly impaired the formation of stable, mature focal adhesions. Yellow arrows, white arrows, short white arrows and asterisks indicate central fibers, transverse arcs, cortical cables and filopodia, respectively.

Fig. S6. GRK2 co-localizes with cortical F-actin in spreading cells. HeLa cells stably over-expressing GRK2 wt (HeLa-wt5), S670A (HeLa-A1) or GRK2-K220R (HeLa-K1) were plated on coverslips coated with fibronectin (10 μ g/ml) for 60 min and fixed for immunofluorescence analysis. Cells were stained for GRK2 and F-actin and analyzed by confocal microscopy. Arrows indicate the leading edge.

Fig. S7. Real-time monitoring of cell adhesion and spreading using the xCELLigence System. (A) Parental or Hela-K1, -A1 and -wt5 cells (12,500 cells) were seeded in 96-well E-plates pre-coated with FN (10 μ M) and allowed to adhere and spread for the indicated times in the presence of 10% FBS. Changes in cell index were measured using the xCELLigence system RTCA SP instrument (Roche) as detailed in Materials and methods. Normalization of the cell index (right panel) was performed to the point at which all cells have reached a plateau in spreading (6h after plating). (B,C) Similar experiments were performed upon down-regulation of GRK2 expression in Hela cells using an adenoviral-GRK2 shRNA construct (B) or upon gene-targeted depletion of GRK2 using MEFs GRK2-flox/flox infected with an adenoviral Cre-recombinase expression vector (C) as described above. Data from representative experiments performed in triplicate are shown. Similar results were obtained in two-additional experiments.

Fig. S8 (A) Identification of GRK2 phosphorylation sites in HDAC6. A battery of GFP-HDAC6 constructs displaying single, double or triple mutations to alanine to target potential serine/threonine residues within the second half of HDAC6 were engineered as detailed in Materials and Methods, considering that GRK2 usually prefers acidic amino acids N-terminal to the phosphorylated residue and hydrophilic residues at P+1. Upon cell expression of the indicated constructs, HDAC6 immunoprecipitates were incubated with recombinant GRK2 in the presence of [γ -³²P] -ATP as detailed in Materials and methods and Figure 3D, followed by SDS-PAGE and analysis for ³²P incorporation by autoradiography (upper panels) or the presence of comparable amounts of HDAC6 or GRK2 by Coomassie staining (lower panels). Mutation to alanine of serine residues 1060/1062 or of residues 1060/1062 and 1069 markedly reduces HDAC6 phosphorylation by GRK2, whereas mutation of serine 458, a reported target for CKII (Watabe and Nakaki, 2011) did not affect GRK2-mediated phosphorylation. (B) Cellular assays using these GRK2 phosphorylation-deficient mutants showed that phosphorylation of HDAC6 at these residues is necessary for full tubulin deacetylase activity. HeLa cells were transfected with the indicated GFP-tagged HDAC6 constructs or empty vector and levels of HDAC6, tubulin and acetylated tubulin (Ac-tubulin) were determined by western blot analysis as in Fig. 1 A. Data are representative of 2 independent experiments.

Fig. S9. Wound-border cells over-expressing GRK2 mutants defective in HDAC6 modulation display aberrant polarization morphology. Parental or HeLa-K1, -A1 and -wt5 cells were plated at near confluence in FN (10mM)-coated 24-well dishes and scrapped. After 16 hours of wound healing, wound-border cells were photographed using an optical microscope. Arrows indicate cell lamellipodia. Although HeLa-A1 cells display some membrane projections, they seem to be collapsed and miss-oriented compared to parental or HeLa-wt5 cells. Consistently, HeLa-A1 cells fail to migrate in a directional way and do not form stable pseudopodia. In contrast, HeLa-K1 cells exhibit a more drastic phenotype, with a total lack of membrane protrusions, paralleled by the absence of cell scattering.

Supplemental Results

GRK2 regulates cell adhesion and cellular spreading by promoting tubulin deacetylation .

We monitored by confocal microscopy the isotropic spreading of HeLa cells that express endogenous or extra wt GRK2 or mutant proteins S670A and K220R on fibronectin-coated surfaces. Spreading of parental and HeLa-wt5 cells progressed in a sigmoidal way with an initial period of low contact area (10min) that includes the lag time for spreading initiation, followed by a period of fast area growth (between 20 and 60 min after plating). Afterward, spreading slowed down and 2h after plating these cells attained an extension area of 548 ± 66 and $513\pm 55 \mu\text{m}^2$, respectively (Fig. 6A). Such spreading kinetics was similar to that reported for HeLa and other adherent cells (Cuvelier et al., 2007; Dubin-Thaler et al., 2008). However, expression of either GRK2-S670A or GRK2-K220R notably altered such normal spreading pattern. The initial phase of cell spreading proceeded in an exponential way, the spreading area 20min after plating being $27\pm 5\%$ and $43\pm 13\%$ higher in HeLa-A1 and HeLa-K1 cells, respectively, compared to cells expressing similar amounts of the wt GRK2 protein (Fig. 6A and B). However, despite such initial enhanced spreading, A1 and K1 cells did not attain a larger final cellular area (2h after plating the surface of HeLa-A1 and HeLa-K1 was 337 ± 75 and $380\pm 31 \mu\text{m}^2$, respectively, versus $548\pm 66 \mu\text{m}^2$ of HeLa). We reasoned that cells expressing such GRK2 mutants might fail to sustain the spreading at later stages, when cell expansion becomes mostly dependent on FA formation and substrate traction forces (Dubin-Thaler et al., 2008). In support of this notion, both HeLa-A1 and -K1 cells

spreading for 60min on FN display a low number of (aberrant) FAs as compared to HeLa or wt GRK2 cells (Fig. S5A), consistent with our previous report showing that expression of GRK2-S670A promotes the loss of FA due to abrogation of the scaffolding function of GIT-1 (Penela et al., 2008). This defect in adhesion could compromise the maintenance of a fully spread area.

The qualitative features of cell spreading in the aforementioned cells were also analyzed by looking at the organization of the actin and tubulin cytoskeleton. In parental and HeLa cells expressing extra wt-GRK2 the MT network, condensed around the nucleus at early times (10min), rapidly expanded to the periphery after 40min of spreading, with a parallel increase in tubulin acetylation (Fig. 6B). Extension of such cells was accompanied by the formation of round membrane protrusions or blebs detected both at early and late stages of spreading (Fig. 6B, and inserts therein). In line with previous reports, actin stress fibers were not observed in the period of fast continuous spreading, but cortical actin cables, central fibers and actin transverse arcs were detected at later stages (60 and 120min of spreading (Fig. 6B and Fig. S5B), together with actin microspikes and filopodia. However, the organization of the MT and actin cytoskeleton was quite different in cells expressing extra GRK2-S670A or –K220R (Fig. 6B, Fig. S6B and description in the main text)

The modulatory role of GRK2 in cell spreading was also investigated by real-time resistance measurements in HeLa cells expressing endogenous or extra wt GRK2, mutant proteins S670A and K220R, or upon endogenous GRK2 downregulation by using either a specific shRNA construct or gene inactivation by Cre-loxP technology, respectively, spread over a FN-coated gold electrode sensor plate, using the XCELLigence system (Roche Applied Science). Cellular impedance was continuously recorded and converted to a cell index (CI) that allows for the assessment of attached cells on the electrodes and sensing of different outputs such as cell proliferation, cell surface coverage or cellular adhesion strength. Cells were plated and allowed to attach and spread for several hours until reaching a stable base-line, when cells are maximally spread out and polarize to adopt their regular shapes (Fig. S7). Such process, which is followed by a lag period before cell growth initiates, takes 6-8 h in both HeLa and HeLa-wt5 cells, while it is markedly reduced to 3h in HeLa-A1 and –K1 cells. Interestingly, CI values at the point of plateau spreading were >2-fold higher in HeLa cells compared to HeLa-A1 or –K1 stable cell lines (Fig.S7), indicating that the later cells are smaller than control cells, in line with data obtained using confocal

microscopy. CI values were normalized to the point at which all cells have reached a plateau in spreading (6h after plating) in order to circumvent cell type-specific differences in absolute CI values. Plotting of normalized CI confirmed that both Hela-A1 and -K1 cells spread more rapidly than Hela-wt5 and control cells, as the slope of the increase in CI was higher in the former cells (Fig. S7). Consistently, the period of time required to achieve such steady-state CI values was significantly lower in Hela-A1, -K1 and -shGRK2 cells, as well as in MEFs GRK2-flox/flox infected with Cre-recombinase (Fig. 7A-B). Interestingly, expression of the HDAC6 S1060,1062, 1069A GRK2-phosphorylation-deficient mutant promoted a cell spreading pattern (Fig. 7F) similar to that observed in the presence of the GRK2 mutants unable to phosphorylate HDAC6 (K220R, S670A) or upon GRK2 downregulation.

Supplemental Materials and methods

Reagents and antibodies

Fibronectin (FN), trichostatin A (TSA) and sodium butyrate (NaB) were purchased from SIGMA, Epidermal Growth Factor Recombinant (EGF) from Calbiochem and Tubacin from Biomol. Bovine GRK2 was purified from baculovirus-infected Sf9 cells as described (Murga et al., 1996). Recombinant GRK2-K220R and GRK2-S670A mutant proteins were kindly provided by Dr. John Tesmer (University of Michigan). Recombinant HDAC6 protein with an N-terminal GST-tag was purchased from Cayman Biochemicals or Abnova (for use in pull down assays). Purified tubulin protein and MAP-rich tubulin were obtained from Cytoskeleton, Inc Urea-treated rod outer segments mainly consisting of rhodopsin were isolated as described previously (Murga et al., 1996). The anti- α -Tubulin (DM1A), anti- α -Tubulin FITC-conjugated and anti-acetylated Tubulin (611B1) monoclonal antibodies and monoclonal antibodies against poly-glutamylated (clone B3) or tyrosinated (clone TUB-1A2) tubulin were purchased from SIGMA. The goat polyclonal anti-Actin (I-19) and anti-HDAC6 (L-18) antibodies as well as the rabbit polyclonal anti-GST (Z-5), anti-GRK2 (C-20), anti-HA epitope (Y-11), ERK1 (C-16), ERK2 (C-14) and anti-SIRT2 (H-95) antibodies were from Santa Cruz. A monoclonal antibody raised against GRK2/3 and cortactin were purchased from Upstate Biotechnology. The acetyl-cortactin polyclonal antibody was obtained from Millipore, the anti-Paxillin monoclonal antibody from BD Transduction Laboratories, the anti-pSer₆₇₀-GRK2 polyclonal antibody from Biosource International, the anti-phospho-ERK1/2 polyclonal from Cell Signaling Technologies and the anti-GFP mouse monoclonal antibody from Roche.

Plasmids

Plasmids encoding mHDAC6-HA wt and HDAC6 truncated mutants (N, N+DD1, DD1, DD2, C+DD2 and C) were kindly provided for Dr. Saadi Khochbin (INSERM, Grenoble, France). The GFP-HDAC6 construct was generously provided for Dr. Francisco Sanchez-Madrid (Instituto de Investigación Sanitaria La Princesa, Madrid, Spain). Plasmids encoding mCherry α -tubulin-wt or mCherry- α -tubulin-K40A (Deribe et al, 2009; Dompierre et al., 2007) were kindly provided by Drs. I. Dikic (Goethe University School of Medicine, Frankfurt, Germany) and F. Saudou (Institut Curie, Orsay, France) with approval from Dr. R.Tsien laboratory. Plasmids for wild-type

cortactin and mutated constructs that mimic the deacetylation (cortactin-K9R) or acetylation (cortactin-K9Q) state of cortactin were generously provided by Dr. E. Seto (Moffit Cancer Research Center, Florida). A GFP-HDAC6 S458A mutant that has been reported to be unable to be phosphorylated by casein kinase II (Watabe and Nakaki, 2011) was made available by Dr. T. Nakaki (Teikyo University, Japan). All other human GFP-HDAC6 serine to alanine phosphorylation mutants were prepared using the Quickchange(R) site-directed mutagenesis kit (Stratagene) and verified by DNA sequencing. The cDNAs encoding GRK2-wt, the catalytically inactive GRK2-K220R mutant and the phosphorylation mutant GRK2-S670A have been previously described in our laboratory (Penela et al., 2008) pEGFP-N1 and pLKO.1-shRNA-GRK2 plasmids were obtained from Clontech and Sigma, respectively.

Down-regulation of GRK2 expression

GRK2 silencing was achieved by RNA interference using either a pLKO.1 plasmid (SIGMA) encoding a shRNA-GRK2 construct or an adenovirus vector (AV.GRK2-shRNA) bearing the target GRK2 shRNA sequence (5'-GCAAGAAAGCCAAGAACAAGC-3'), using an un-related vector expressing lamin shRNA (AV. LAM shRNA) as control as previously described (Penela et al., 2008). Primary MEFs were infected either with AV.GRK2-shRNA or its control at 50 pfu/cell and cells were analyzed for migration and signaling 72 hours post-infection. Gene-conditional depletion of GRK2 was achieved in primary MEFs derived from GRK2-flox/flox mice (gently provided by Dr. W.J Koch, Thomas Jefferson University, Philadelphia USA) infected with adenovirus expressing the Cre- recombinase, Ad5Cre (Gene Transfer Vector Core, University of Iowa) or its control at 100pfu/cell and cells were analyzed for migration, spreading and tubulin acetylation 48h post-infection. For stable silencing of GRK2, HeLa cells were co-transfected with pEGFP-C1 and pLKO.1-siRNA-GRK2 plasmids and GFP positive cells (>90%) were selected using the FACS Vantage cell sorter (BD Biosciences). For monitoring the efficiency of GRK2 down-regulation, protein expression was routinely measured by immunoblotting in whole cell lysates.

Western blotting, immunoprecipitation and kinase phosphorylation assays

Western blot analysis was performed using post-nuclear supernatants (10-40 µg of protein) derived from cells lysed in ice-cold RIPA buffer (50 mM Tris-HCl, pH 7.5, 300 mM NaCl, 1% Triton-X, 0,1% SDS, 0,5% sodium deoxycholate, 50 mM NaF, 0.1 mM sodium orthovanadate, 1 mM PMSF, 2.5 mM benzamidine, and 2 µg of aprotinin per

ml). Immunoblots were developed and quantified using IR680 or 800 labelled secondary antibodies (Licor) with the Odyssey Infrared Imaging System (Li-Cor) or with peroxidase-conjugated anti-IgG antibodies using a chemiluminescence method (ECL, Amersham Pharmacia Biotech, UK). When required, bands were quantified by laser-scanner densitometry.

For investigating endogenous co-immunoprecipitation of GRK2 and HDAC6, cytoplasmatic extracts from HeLa cells lysates were prepared in a hypotonic buffer (20mM Hepes pH 7.5; 10mM MgCl₂; 1mM NAF; 0.1 MM EDTA; 1 mM sodium orthovanadate, 1 mM PMSF, 2.5 mM benzamidine, and 2 µg of aprotinin per ml) and, after centrifugation (2,000rpm), the supernatants were diluted in immunoprecipitation buffer (50 mM Tris-HCl, pH 7.5, 150 mM NaCl, 0.1% Triton-X, 0.5 mM EDTA, 50 mM NaF, 0.1 mM sodium orthovanadate, 1 mM PMSF, 2.5 mM benzamidine, and 2 µg of aprotinin per ml) and incubated in the presence of 5 micrograms of either HDAC6 (H-300) antibody or IgG. For other immunoprecipitation assays, 250-500 µg of protein from whole-cell lysates were incubated with 20 µl of an agarose conjugated-anti-HA antibody (sc-7392 AC) for 4 h at 4°C, or 16 hours with primary antibody followed by 2 hours of incubation with protein G/Agarose (Sigma). The beads were then washed 5 times in IP buffer (see above) and analyzed by immunoblotting or further equilibrated in kinase buffer for kinase assays (see below). The amount of co-precipitated protein was normalized to the amount of the immunoprecipitated protein, as assessed by the specific antibodies.

For kinase assays, recombinant GRK2-wt or mutant GRK2-K220R or GRK2-S670A proteins (100, 50 or 12.5 nM) were mixed in kinase buffer (20 mM Hepes pH 7.2, 2 mM EGTA, 1 mM sodium orthovanadate, 1 mM DTT, 1 mM NaF, 20 mM MgCl₂, 10 mM glycerol-phosphate, 100 µM ATP, 4,000 cpm/pmol [³²P]-ATP) with either purified human GST-HDAC6 at the concentrations indicated or with immunoprecipitated tagged full-length, mutant or truncated constructs of HDAC6 expressed in cells. Purified rhodopsin (25 nM) or tubulin (100 nM) were also assessed as positive control substrates. After 30 min of incubation at 30° C, the reactions were stopped by adding 10 µl of 4x sample buffer, and samples were analyzed by SDS-PAGE electrophoresis. The gels were stained with Coomassie and subjected to autoradiography for 4 to 24 h.

Immunofluorescence and confocal microscopy

Cells previously kept or not in suspension and seeded onto FN (10 µg/ml)-coated coverslips for different times were rinsed in phosphate-buffered saline (PBS), fixed in 4% paraformaldehyde for 30 min and washed again with PBS. Non-specific sites were blocked by incubation with PBS containing 1% BSA and 0.5% Triton-X100 for 1 h at room temperature. Cells were then washed 4 times with PBS and incubated 1 h with anti-HDAC6 polyclonal antibody (1:250), with anti-GRK2(p-S670) (1:100) or with anti-GRK2 (dilution 1:200), anti- α Tubulin-FITC conjugated (Sigma, 1:2000), anti-Acetylated Tubulin (Sigma, 1:500) and anti-Paxilin (1:500) monoclonal antibodies. F-actin was stained with phalloidin-Alexa594 (dilution 1/150). After washing with PBS, cells were incubated for 1 h with Alexa Fluor 488 and 594 secondary antibodies (1:500, Molecular Probes) and mounted in mowiol. Samples were examined by confocal microscopy.

GST Pull-down assays

For GST pull-down assays, GST-HDAC6 (400ng) or GST (400ng) purified proteins were incubated with recombinant GRK2 (200 ng) in immunoprecipitation buffer (see above) for 90 min at 4° C in the presence or absence of purified MAP-rich-Tubulin (5µg) as indicated. After addition of glutathione-Sepharose 4B (Pharmacia Amersham Biotech) for 45 min, precipitated complexes were washed and eluted with SDS sample buffer. Bound GRK2 or tubulin were analyzed by immunoblotting using specific antibodies.

Transwell and wound healing migration assays

MEFs isolated from either GRK2-flox/flox, GRK2 +/- or wild-type (WT) mice and parental and Hela-wt5 cells sorted upon co-transfection with CD8 and different tubulin or cortactin constructs were seeded (30,000 cells/well) onto fibronectin-coated (20 µg/ml) 6.5-mm Transwell filters with 8-µm pores (Costar) after being serum-starved in 0.1% FBS-containing medium. HDAC inhibitors were added 30 min before the migration assay and maintained thereafter by addition to the upper and bottom cell chamber. After approximately 5 hours of migration, cells were fixed and stained with 5 µg/ml DAPI. Five random fields of each filter were counted. For wound-healing assays, parental Hela cells and stable cell lines Hela-wt5, Hela-K1 or Hela A1 were plated at sub-confluence on fibronectin-coated 24-well plates. After 24 hours of incubation, cells were scratched with a micropipette tip. Just after scratch (time 0) and 16 hours later, cell migration was observed with an Olympus IX51 inverted microscope equipped with a

CCD camera.

Morphometric Cell Analysis

Cultures were analyzed on a Zeiss 510 confocal microscope (Carl Zeiss, Heidelberg, Germany). A set of high-resolution digital images of parental HeLa cells, stable cell lines HeLa-wt5, HeLa-A1, HeLa-K1 and HeLa-shGRK2 or cells transiently expressing phospho-defective HDAC6 mutants allowed to spread for different times was recorded at a resolution of 7.20 pixels per μm . Image processing and measurement steps were performed in the public domain software for image analysis ImageJ (NIH, Bethesda, Maryland, USA; <http://rsb.info.nih.gov/ij/>). Morphometric analysis included measurement of the average cell area. Fifteen unbiased-selected cells were measured on 10 different fields (objective x63) for each cell type and condition. Cell area was measured using the ImageJ's thresholding tool and intensity values (maximum, minimum and average) were obtained for each cell. Average values from all of the cells within a field were pooled for subsequent plotting and analysis.

Real time monitoring of cell spreading

To monitor the process of spreading in live cells at real-time, we measured in parallel changes in cellular electrical impedance using the xCELLigence system (Roche Applied Science). HeLa cells and control or Cre-infected MEFs GRK2-flox/flox were trypsinized and resuspended in DMEM containing 10% fetal bovine serum. 12,500 cells per condition were seeded onto a 96-well microtiter xCELLigence assay plate (E-Plate) (ACEA Biosciences Inc.) and placed on the Real-time xCELLigence Cell Analyzer platform (Roche Applied Science) at 37 °C for recording impedance measurements every 5 min. The cell index (CI) unit is defined as $(R_n - R_b)/15$, where R_n is the cell electrode impedance of the well when it contains cells, and R_b is the background impedance of the well with media alone. The data were represented as the time needed to complete total spreading of the cell.

Supplemental References

Deribe YL, Wild P, Chandrashaker A, Curak J, Schmidt MH, Kalaidzidis Y, Milutinovic N, Kratchmarova I, Buerkle L, Fetchko MJ, Schmidt P, Kittanakom S, Brown KR, Jurisica I, Blagoev B, Zerial M, Stagljjar I, Dikic I (2009) Regulation of epidermal growth factor receptor trafficking by lysine deacetylase HDAC6. *Sci Signal* 2(102): ra84

Dompierre, J.P., Godin, J.D., Charrin, B.C., Cordelières, F.P., King, S.J., Humbert, S. and Saudou, F. (2007) Histone deacetylase 6 inhibition compensates for the transport deficit in Huntington's disease by increasing tubulin acetylation. *J. Neurosci.* 28, 3571-3583.

Hubbert, C., Guardiola, A., Shao, R., Kawaguchi, Y., Ito, A., Nixon, A., Yoshida, M., Wang, X.F., and Yao, T.P. (2002). HDAC6 is a microtubule-associated deacetylase. *Nature* 417, 455-458.

Cho, S.Y. and Klemke, R.L. (2002). Purification of pseudopodia from polarized cells reveals redistribution and activation of Rac through assembly of a CAS/Crk scaffold. *The Journal of cell biology* 156, 725-736.

Murga, C., Ruiz-Gomez, A., Garcia-Higuera, I., Kim, C.M., Benovic, J.L., and Mayor, F., Jr. (1996). High affinity binding of beta-adrenergic receptor kinase to microsomal membranes. Modulation of the activity of bound kinase by heterotrimeric G protein activation. *The Journal of biological chemistry* 271, 985-994.

Penela, P., Ribas, C., Aymerich, I., Eijkelkamp, N., Barreiro, O., Heijnen, C.J., Kavelaars, A., Sanchez-Madrid, F., and Mayor, F., Jr. (2008). G protein-coupled receptor kinase 2 positively regulates epithelial cell migration. *The EMBO journal* 27, 1206-1218.

Watabe M, Nakaki T (2011) Protein kinase CK2 regulates the formation and clearance of aggresomes in response to stress. *J Cell Sci* 124, 1519-1532

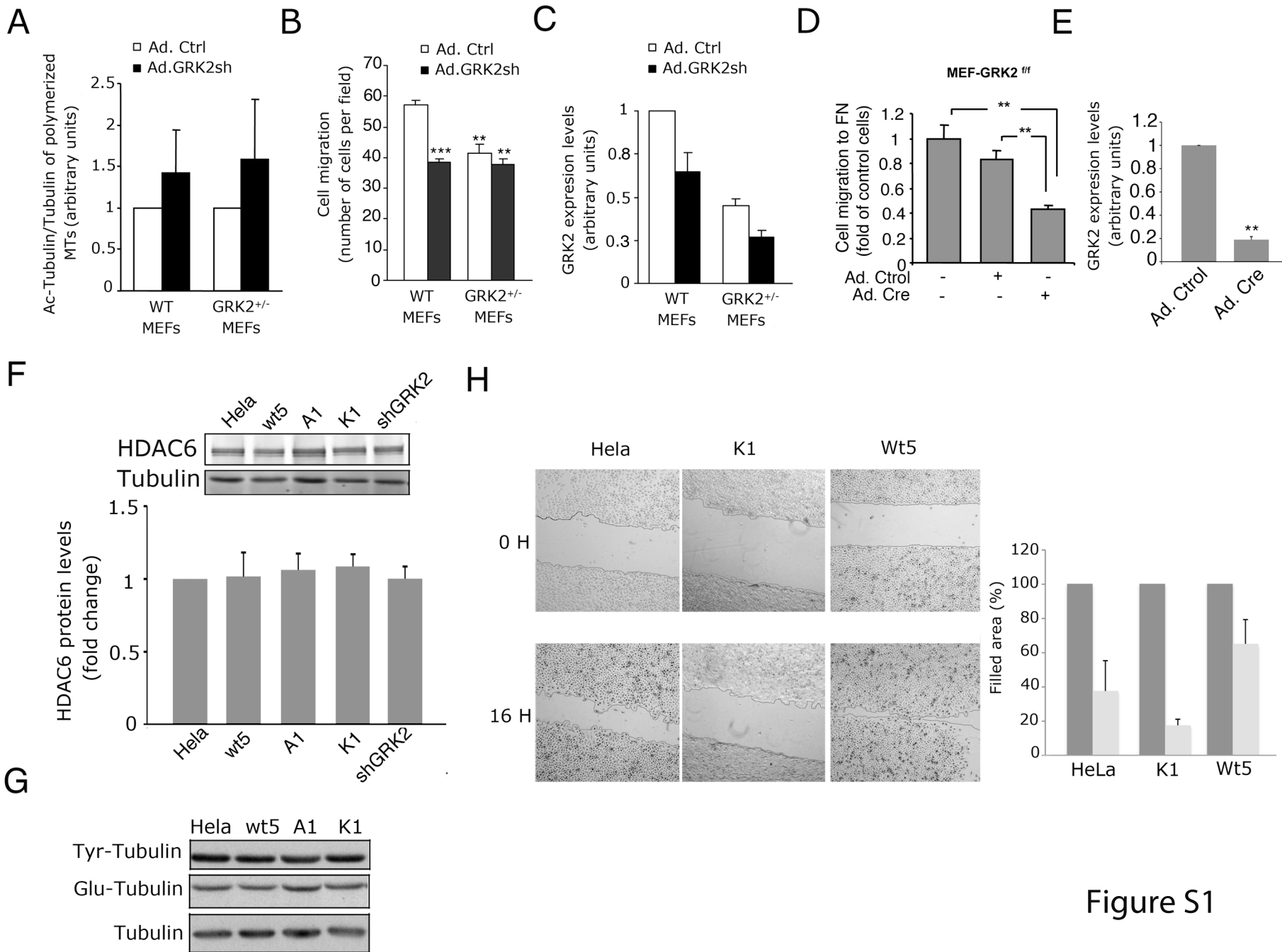
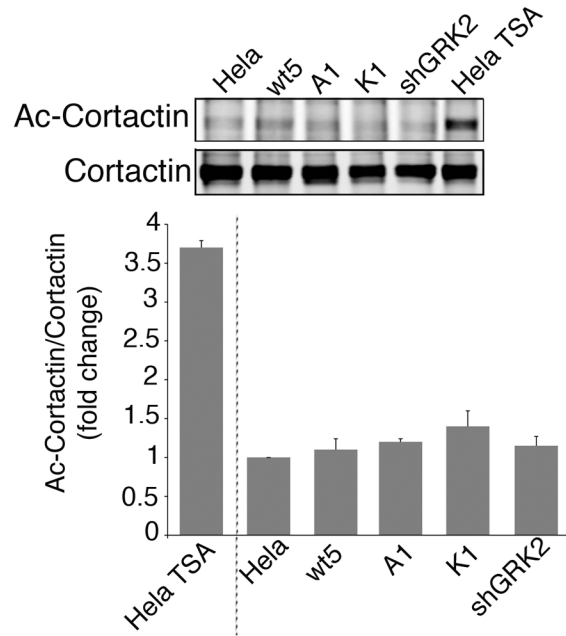
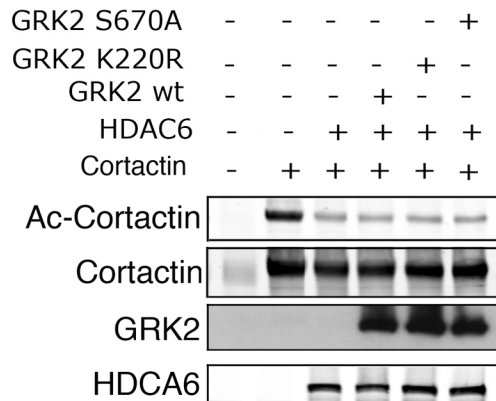


Figure S1

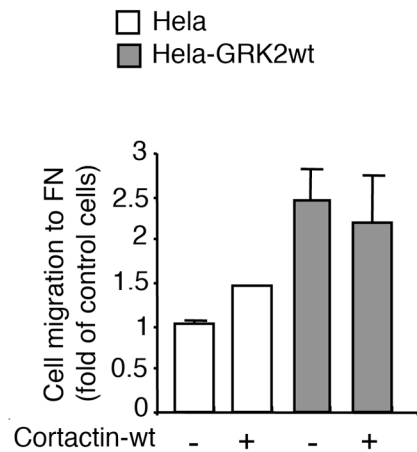
A



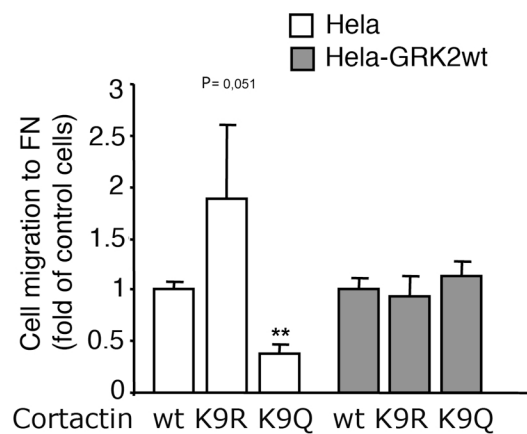
B



C



D



E

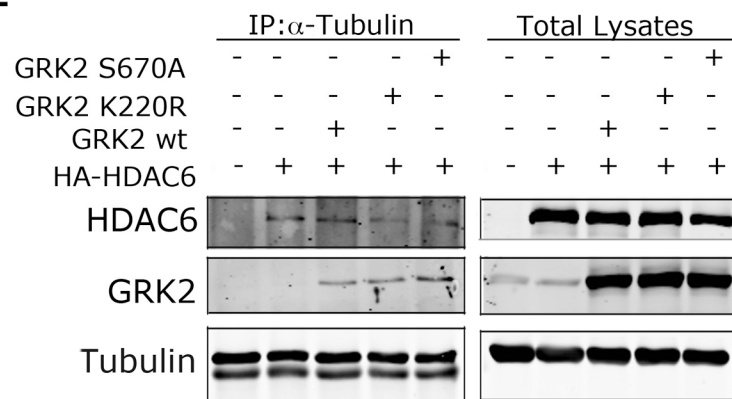
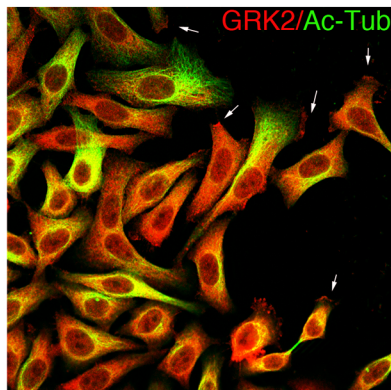
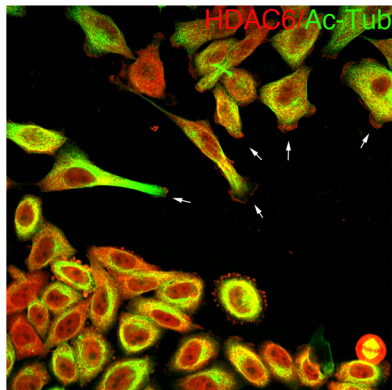


Figure S2

A



B

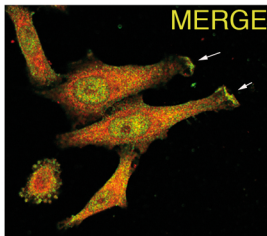
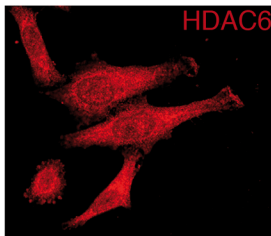
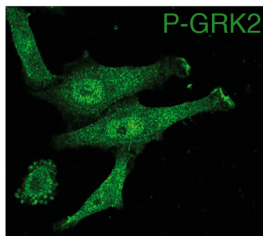


Figure S3

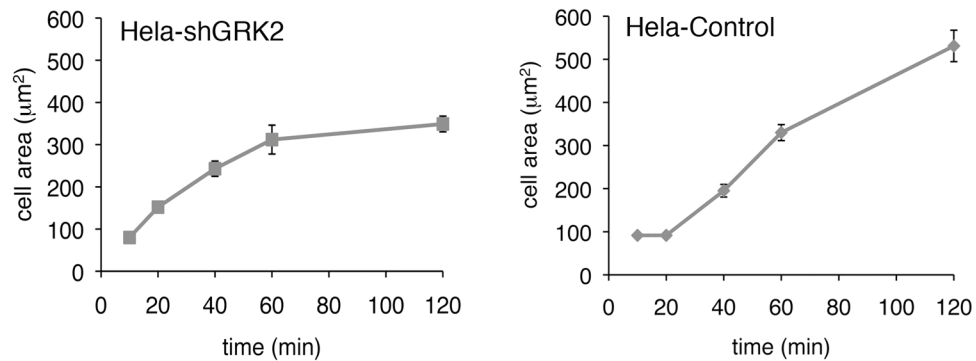
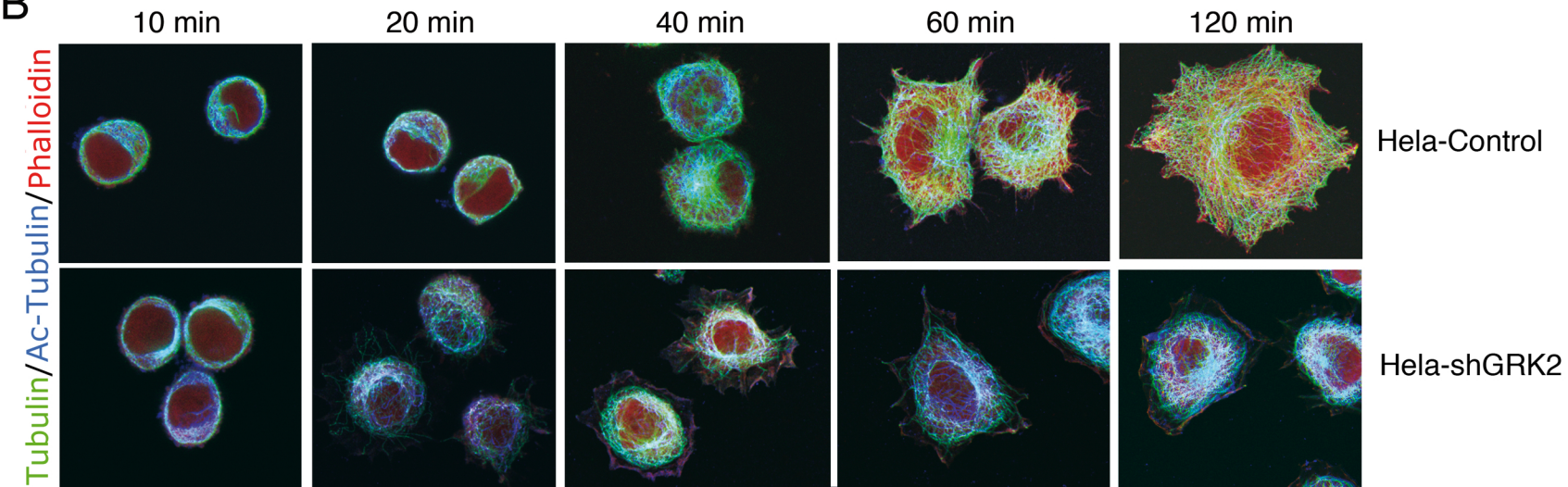
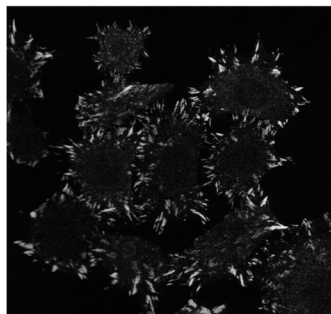
A**B**

Figure S4

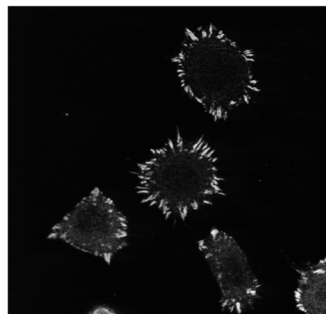
A

Paxilin staining

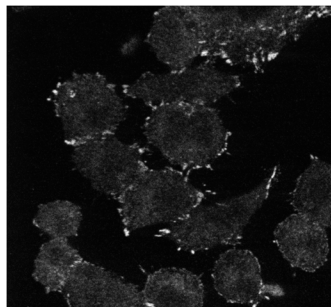
Hela



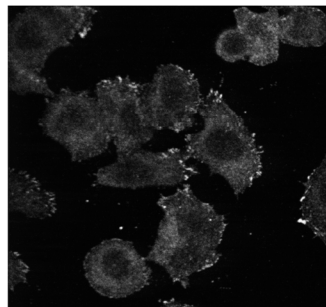
wt5



K1



A1

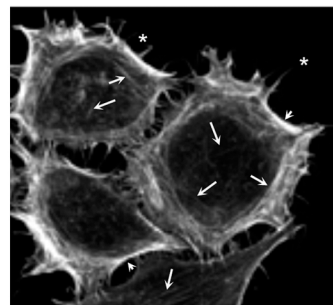


60 min of spreading

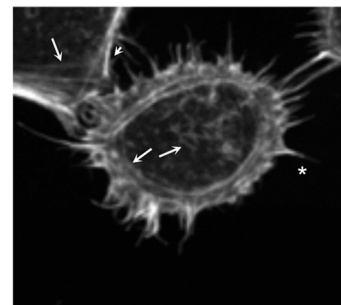
B

F-actin staining

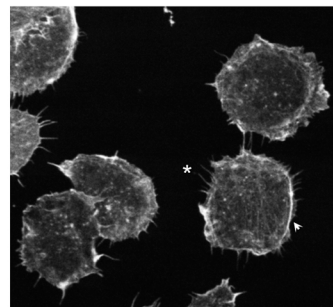
HeLa



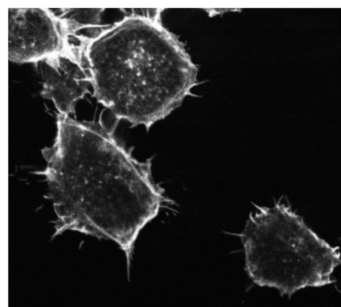
wt5







A1



K1



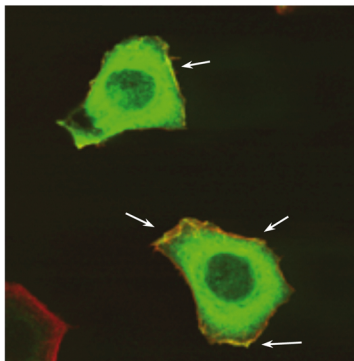
-  Central fibers
-  Transverse arcs
-  Cortical cables
-  Filopodia

60 min of spreading

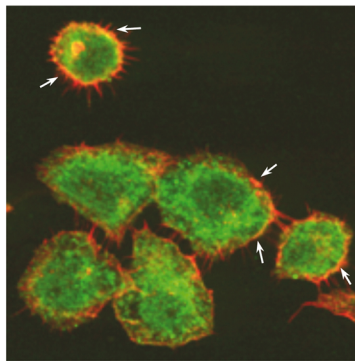
Figure S5

GRK2/Actin staining

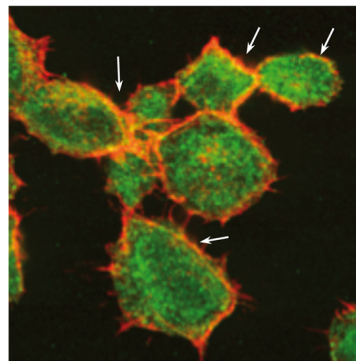
wt5



A1

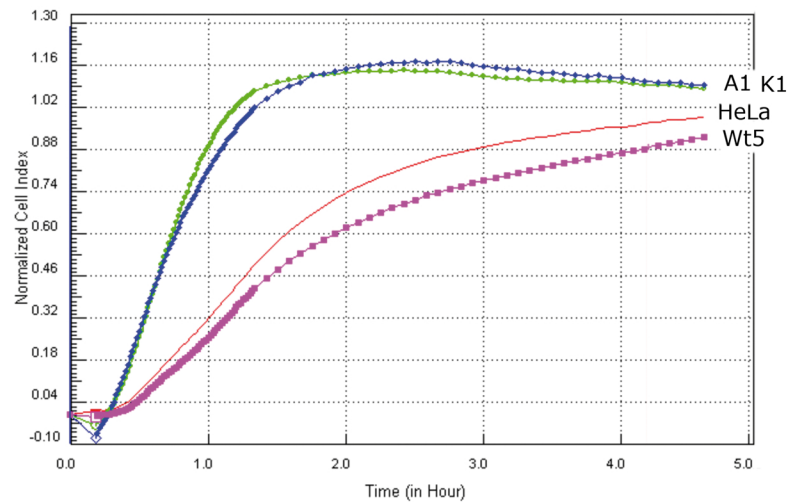
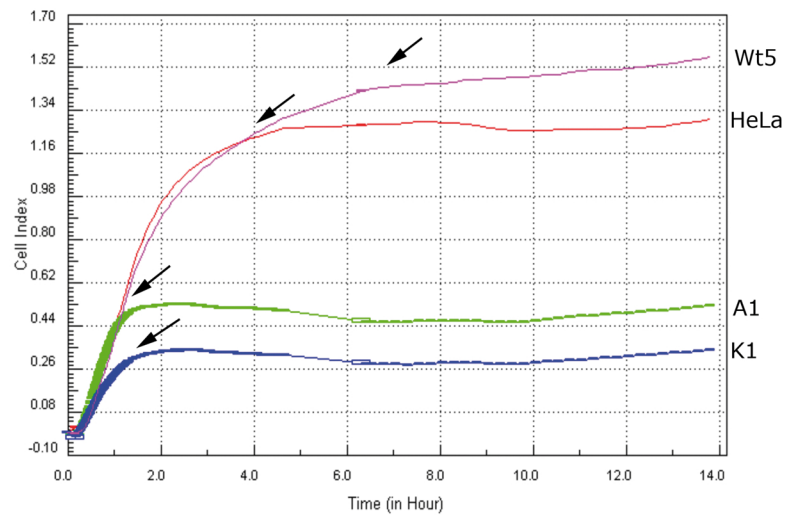
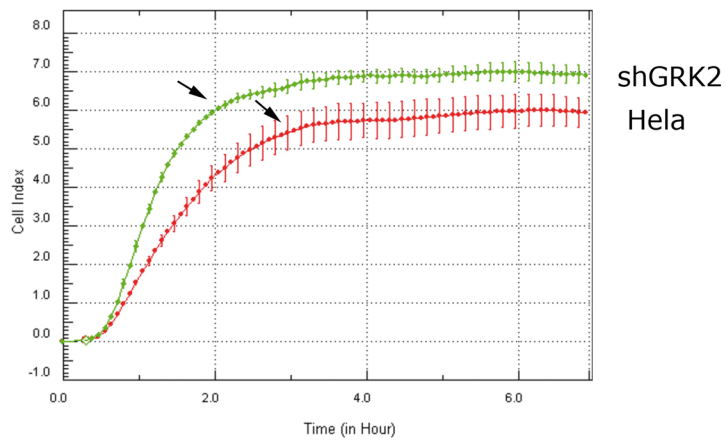
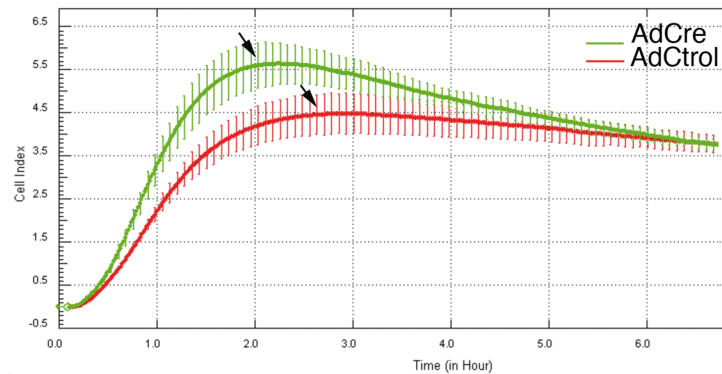


K1

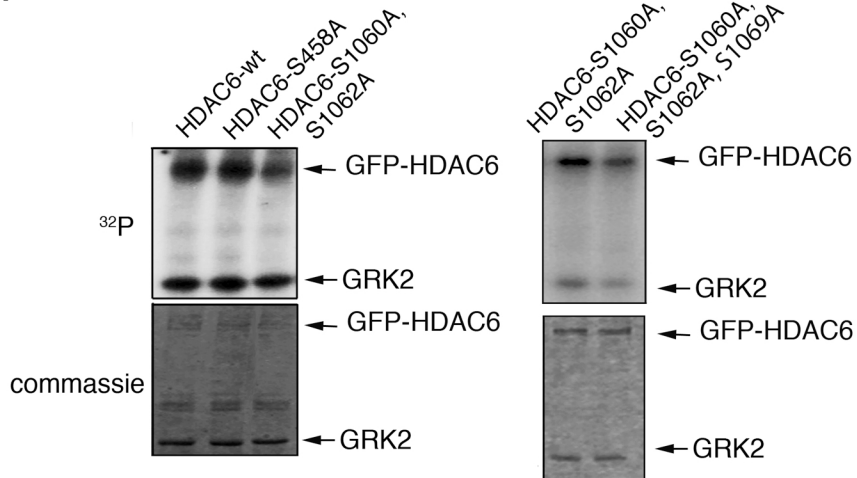


60 min of spreading

Figure S6

A**B****C****Figure S7**

A



B

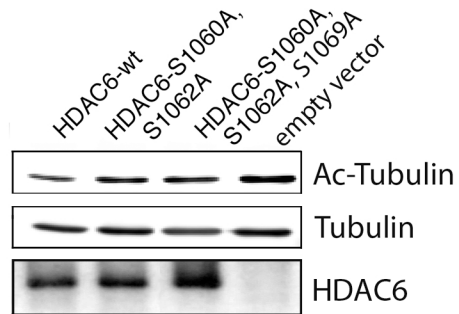
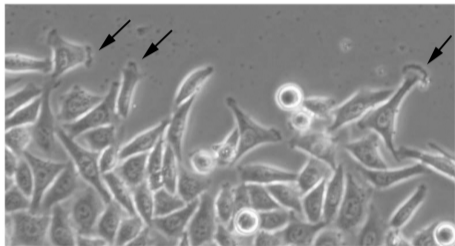
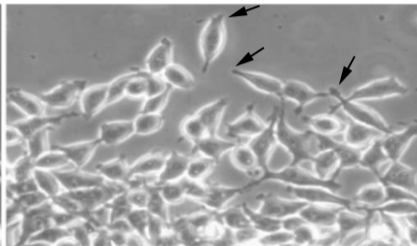


Figure S8

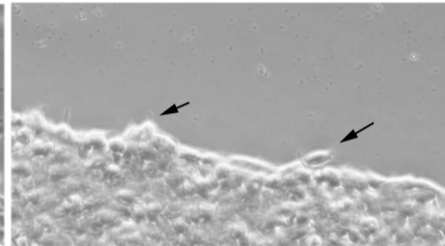
HeLa



A1



K1



wt5

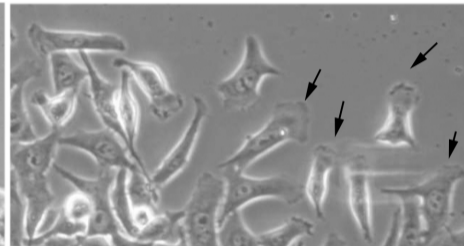


Figure S9